

## Characterizing Spatiotemporal Variability in Phosphorus Export across the United States through Bayesian Hierarchical Modeling

Kimia Karimi\* and Daniel R. Obenour



Cite This: *Environ. Sci. Technol.* 2024, 58, 9782–9791



Read Online

ACCESS |

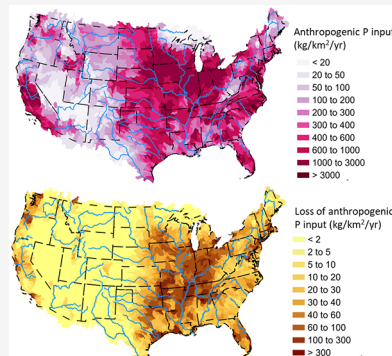
Metrics & More

Article Recommendations

Supporting Information

**ABSTRACT:** Phosphorus inputs from anthropogenic activities are subject to hydrologic (riverine) export, causing water quality problems in downstream lakes and coastal systems. Nutrient budgets have been developed to quantify the amount of nutrients imported to and exported from various watersheds. However, at large spatial scales, estimates of hydrologic phosphorus export are usually unavailable. This study develops a Bayesian hierarchical model to estimate annual phosphorus export across the contiguous United States, considering agricultural inputs, urban inputs, and geogenic sources under varying precipitation conditions. The Bayesian framework allows for a systematic updating of prior information on export rates using an extensive calibration data set of riverine loadings. Furthermore, the hierarchical approach allows for spatial variation in export rates across major watersheds and ecoregions. Applying the model, we map hotspots of phosphorus loss across the United States and characterize the primary factors driving these losses. Results emphasize the importance of precipitation in determining hydrologic export rates for various anthropogenic inputs, especially agriculture. Our findings also emphasize the importance of phosphorus from geogenic sources in overall river export.

**KEYWORDS:** watershed modeling, nutrients, pollution, hydrologic losses, geogenic sources



### 1. INTRODUCTION

Nutrient inputs to inland and coastal waters have increased substantially over the past century, causing eutrophication that contributes to various water quality problems.<sup>1,2</sup> Phosphorus (P), in particular, is recognized as a limiting nutrient of algal growth for many lakes and reservoirs.<sup>3–5</sup> Developing efficient watershed management strategies to reduce eutrophication relies on estimating riverine nutrient export and linking it with anthropogenic nutrient inputs.<sup>6,7</sup> The ability to characterize P export and understand its interannual variability over large geographic areas can improve nutrient management at a national or continental scale.

Various models have been developed to estimate P export across different spatial and temporal scales. They also provide opportunities to explore variability in the sources and processes controlling watershed export. Recent large-scale studies have used empirical models (e.g., multiple linear regression) to explore factors influencing riverine nutrient export. This approach has been used for modeling total nitrogen (TN) export across the contiguous United States (CONUS)<sup>6</sup> and for both total phosphorus (TP) and TN across China.<sup>8</sup> These studies found that spatial variability in export is primarily driven by nutrient inputs, while interannual variability is dominated by precipitation. While these studies produce substantial insights through linear regression, the ability to incorporate nonlinear parametrizations and regional

variability in parameters (i.e., rate coefficients) could potentially improve model accuracy and interpretation.<sup>9</sup>

Watershed nutrient transport models that apply simple, process-based formulations using data-driven, statistical calibration techniques are often referred to as “hybrid” models.<sup>10</sup> As an example, the Spatially Referenced Regressions of Contaminant Transport on Watershed Attributes (SPARROW) uses nonlinear regression to relate watershed characteristics (that affect nutrient export and retention) to instream nutrient load estimates.<sup>11</sup> SPARROW has been applied across CONUS to predict riverine nutrient loads and characterize subregions dominated by point and nonpoint sources.<sup>11,12</sup> However, SPARROW is based on static hydrologic and development conditions, which largely precludes it from predicting temporal variability. Recent hybrid models have incorporated precipitation-driven interannual variability into TP export predictions, but these studies were developed at relatively small spatial scales.<sup>13,14</sup>

A key consideration when developing nutrient export models over large areas is whether the governing parameters

Received: September 11, 2023

Revised: May 7, 2024

Accepted: May 8, 2024

Published: May 17, 2024



ACS Publications

© 2024 American Chemical Society

9782

<https://doi.org/10.1021/acs.est.3c07479>  
*Environ. Sci. Technol.* 2024, 58, 9782–9791

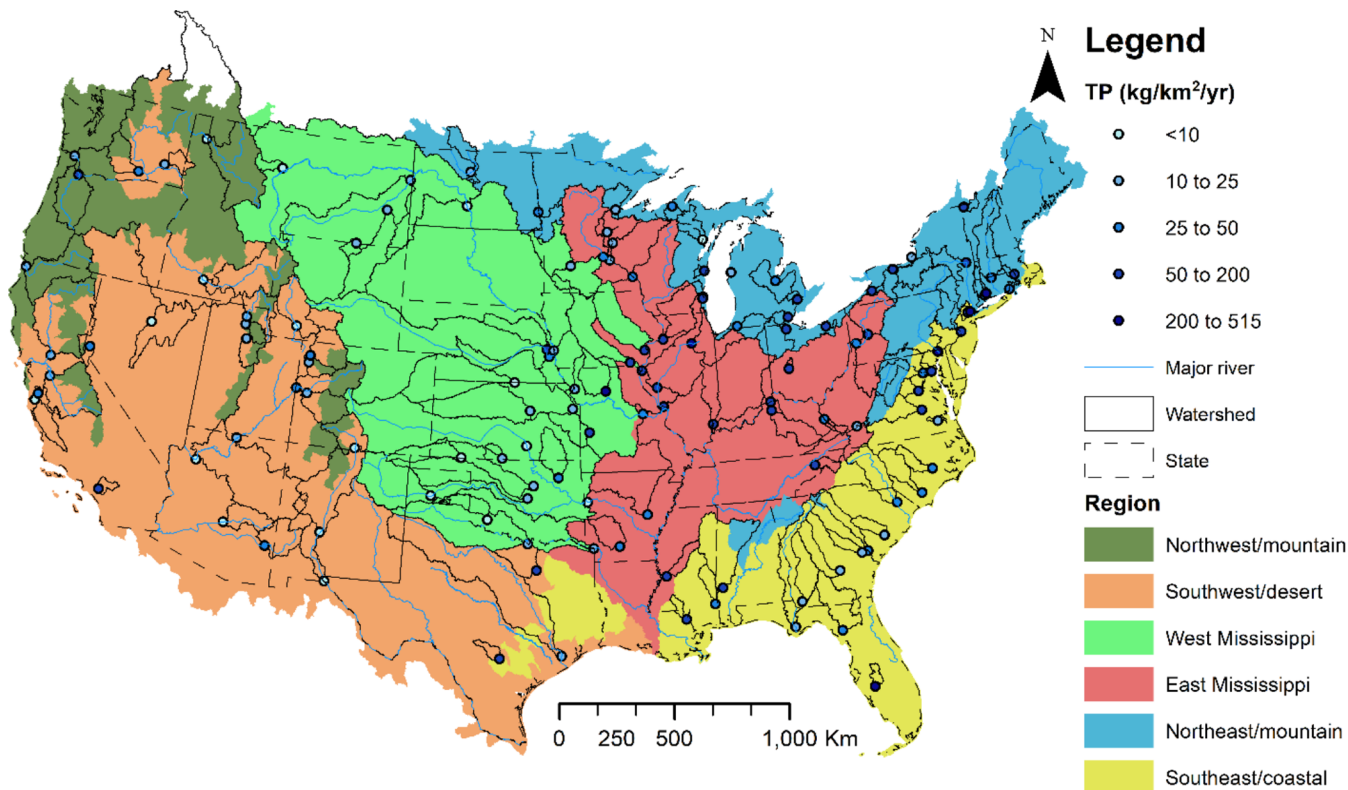


**Figure 1.** Map of 131 load monitoring sites (LMSs) used in this study, their corresponding watersheds, and estimated mean TP export ( $\text{kg}/\text{km}^2/\text{yr}$ ). The six regions defined for model development are also shown. Note that individual LMS watersheds were assigned to the region of maximum overlap.

should vary regionally to account for potential spatial heterogeneity in nutrient sources and watershed processes, beyond what is reflected in available input data sets and model formulations. Improvements in the accuracy of national TN and TP SPARROW models were demonstrated by using regionalized model parameters, but this regionalization also increased parameter uncertainties compared to a uniform national model.<sup>10</sup> The authors noted that a hierarchical approach<sup>15</sup> may be beneficial for improving model performance in this case. In a hierarchical framework, regionally varying model parameters are treated as members of a common statistical distribution, which helps constrain parameter estimates and their uncertainties, especially for regions with relatively sparse calibration data.<sup>16</sup> In addition, hierarchical models are often developed in a Bayesian framework via Markov Chain Monte Carlo sampling,<sup>17</sup> allowing for flexibility in the model formulation (e.g., nonlinear parametrizations), multiple levels of random effects, systematic incorporation of prior knowledge (e.g., from the scientific literature), and rigorous uncertainty quantification.<sup>18</sup>

Here, for the first time, spatial and interannual variability in TP export is modeled across the entire CONUS. To accomplish this, we develop and apply a parsimonious hybrid model of watershed P loading and retention. Through Bayesian inference, we characterize P export rates from agricultural inputs, urban inputs, and geogenic sources under varying precipitation conditions. In addition, a hierarchical formulation allows key rates to vary spatially to improve predictive accuracy and reveal regional differences in P export. We also apply the model to map TP export across CONUS under varying precipitation conditions.

## 2. METHODS

**2.1. Estimation of Riverine P Loads.** Estimates of riverine TP export are critical for hybrid model calibration. We identified 131 load monitoring sites (LMSs) based on proximity to the outlet of U.S. Geological Survey (USGS) Hydrologic Unit Code 4 (HUC4) watersheds. Each LMS has 90+ TP samples for 1997–2017 (Figure 1, and Supporting Information, S1). Streamflow data were obtained mainly from federal gaging stations.<sup>19,20</sup> Water quality data were obtained from the Water Quality Portal,<sup>21</sup> which includes USGS and state monitoring program data, and from the NCWQR Tributary Loading portal.<sup>22</sup>

Flow and TP concentration data were used to develop annual TP loading estimates. As TP concentrations were infrequently sampled, we used the Weighted Regressions on Time, Discharge, and Season (WRTDS)<sup>23</sup> approach to impute missing concentrations and develop estimates of annual TP load. We focused on water-year loads (Oct–Sep) on account of the delay between winter (and late fall) snow accumulation and runoff in the following calendar year. Our objective was to develop estimates of the annual TP load for 2002–2012 at each LMS. However, years with missing flow records or no TP observations were omitted from this study. TP loads were normalized by watershed area to determine TP export ( $\text{kg}/\text{km}^2/\text{yr}$ ). LMS watershed delineations were obtained from the USGS GAGES-II database<sup>24</sup> and StreamStats.<sup>25</sup>

**2.2. Development of P Input Data.** Anthropogenic P inputs were obtained from a recent national inventory.<sup>26</sup> In this study, agricultural inputs include the summation of farm fertilizers, pesticides, herbicides, and livestock waste. Urban fertilizers (typically a nonpoint source) and urban human/

household wastes (typically mitigated through onsite or municipal wastewater treatment) are treated separately. Note that “urban” sources also include household inputs in rural areas, though these are relatively small. Atmospheric deposition (<2% of P inventory<sup>26</sup>) was not considered an additional input as it represents a somewhat localized redistribution of P rather than an original source.<sup>27</sup> The inputs were available for 2002, 2007, and 2012 at the HUC8 watershed scale<sup>26</sup> and aggregated to the LMS watershed scale for model fitting. In cases where HUC8 watersheds were not completely within an LMS watershed (i.e., around the LMS outlet), the HUC8 inventory components were apportioned using land cover available for 2002 and 2012 and population data for 2000 and 2010.<sup>28,29</sup> Agricultural land cover was used to apportion agricultural inputs, the urban land cover was used to apportion urban fertilizers, and population was used to apportion human waste. For HUC8 watersheds in Canada or Mexico, the land use data for 2005, 2010, and 2015 were used, assuming the same input rates as in the U.S. portion of the LMS.<sup>30</sup> P inputs were first determined for each inventory year, and then interpolated linearly between years (Figure S1–2).

Background P in soils is another potential source of watershed P export. We used C-horizon P concentrations from USGS,<sup>31</sup> which are expected to reflect geogenic (i.e., parent) material.<sup>32</sup> While C-horizon P concentrations may be modestly elevated in some agricultural lands (i.e., by ~90 ppm in the Midwest), geologic drivers of variability in the C-horizon are much greater.<sup>32</sup> Soil P concentrations were spatially interpolated (inverse-distance weighting), and spatial averages were obtained for each HUC8 and LMS watershed (Figure S1–3).

**2.3. Precipitation and Waterbody Data.** Precipitation was integrated into the model formulation to account for temporal variability in TP export. Monthly downscaled precipitation data for 1970 to 2018 at a HUC12 watershed scale were obtained from LAGOS-US.<sup>33,34</sup> Monthly values were aggregated to the water year and averaged over HUC8 and LMS watersheds for modeling purposes (Figure S1–4).

Waterbody data were included in the model formulation for P retention. Inland waters were identified from land cover data for 2002 and 2012 (Figure S1–6).<sup>29</sup> Estimates for intervening years were determined through linear interpolation.

**2.4. Hybrid Model Development.** The hybrid model relates the WRTDS-estimated TP export ( $y_{i,t}$ ) of watershed  $i$  in year  $t$  to a combination of deterministic and stochastic components

$$\ln(y_{i,t}) \sim N(\ln(\hat{y}_{i,t}) + \alpha_i, \sigma_{e(j)}) \quad (1)$$

where  $\hat{y}_{i,t}$  is the deterministic TP export prediction ( $\text{kg}/\text{km}^2/\text{yr}$ ). The remaining components of eq 1 are stochastic;  $\alpha_i$  is a normally distributed watershed-level random effect with standard deviation (SD)  $\sigma_{\text{LMS}}$ . The residuals are normally distributed with SD,  $\sigma_{e(j)}$ , that varies hierarchically by region  $j$ ,  $\sigma_{e(j)} \sim N(\mu_{\text{res}}, \tau_{\text{res}})$ . Here,  $\mu_{\text{res}}$  and  $\tau_{\text{res}}$  are the mean and SD of the hyperdistribution. Parameter  $\sigma_{\text{LMS}}$  primarily accounts for spatial stochasticity (among LMS watersheds), and  $\sigma_{e(j)}$  primarily accounts for temporal stochasticity (within LMS watersheds).

The deterministic prediction is the summation of various loading contributions multiplied by a waterbody retention term

$$\hat{y}_{i,t} = (L_{i,t,a} + L_{i,t,uf} + L_{i,t,uh} + L_{i,t,s}) \times e^{(-\kappa \times W_{i,t})} \quad (2)$$

where  $L_{i,t,a}$  is agricultural export,  $L_{i,t,uf}$  is urban fertilizer export,  $L_{i,t,uh}$  is urban human/household waste export, and  $L_{i,t,s}$  is geogenic P export. In addition, as waterbodies are expected to retain P through settling as a first-order process,<sup>14,35,36</sup>  $W_{i,t}$  is the fraction of the watershed area classified as water and  $\kappa$  is a retention coefficient.

The loading contribution from each source type,  $x$  {a, uf, uh, s}, is determined as

$$L_{i,t,x} = I_{i,t,x} \times \beta_x \times \delta_{j(i)} \times (p_{i,t}^{\psi_{j(i)} \times \gamma_x}) \quad (3)$$

where  $I_{i,t,x}$  is the source magnitude with units of  $\text{kg}/\text{km}^2/\text{yr}$  for agricultural and urban inputs and ppm (i.e., mg TP per kg soil) for geogenic soil P. Agricultural and urban ECs ( $\beta_x$ ) represent the fraction of inputs that are exported to rivers and waterbodies (unitless). For background soil, the EC represents the export rate ( $\text{kg}/\text{km}^2/\text{yr}$ ) per unit soil P (ppm). Also,  $\delta_{j(i)}$  is a normally distributed EC-adjustment factor that varies hierarchically by region  $j$ ,  $\delta_{j(i)} \sim N(1.0, \sigma_{\delta})$ .

To account for precipitation impacts on P export, variable  $p_{i,t}$  is the scaled precipitation (unitless), defined by dividing the annual precipitation of watershed  $i$  in year  $t$  by the long-term (1970–2018) mean precipitation of each region. Parameter  $\gamma_x$  is the source-specific precipitation impact coefficient (PIC, unitless), and  $\psi_{j(i)}$  is a normally distributed PIC-adjustment,  $\psi_{j(i)} \sim N(1.0, \sigma_{\psi})$ .

Region boundaries were defined using level I and II ecoregions (<https://www.epa.gov/eco-research/ecoregions>) and major river basins (Figure 1). The Mississippi River Basin (MRB) was separated into western and eastern regions, corresponding to ecoregions 9 and 8, respectively. The southeast/coastal region consists of ecoregions 8.3 and 8.5 (outside of the MRB), and the northeast/mountain includes the remaining portions of ecoregions 8 and 5 and a small northern portion of ecoregion 9. The northwest/mountain region includes ecoregions 6 and 7, and the southwest/desert region includes ecoregions 10, 11, 12, 13, and the remainder of ecoregion 9.

**2.5. Bayesian Inference and Model Assessment.** Model parameters were estimated through Bayesian inference, updating prior knowledge based on the model formulation and riverine P export estimates. Prior distributions for ECs were generally derived from Preston et al.,<sup>9</sup> who provided a synthesis of six regional SPARROW models throughout CONUS. Priors for PICs are mildly informative, being loosely based on Karimi et al.,<sup>13</sup> who used a similar parametrization for precipitation in a hybrid model of North Carolina watersheds. Additional details on priors are provided in Supporting Information (S2).

Bayesian inference was conducted through Hamiltonian Monte Carlo sampling<sup>37</sup> using Rstan<sup>38</sup> in R.<sup>39</sup> Three parallel chains were run for 10,000 iterations, and the first 1000 were discarded as burn-in. Then, by selecting every fifth iteration (to reduce autocorrelation), 5400 samples characterize the joint posterior parameter distribution. Chain convergence was considered achieved when the scale reduction coefficient was below 1.1.<sup>17</sup>

Model performance was evaluated by comparing predicted and WRTDS-estimated loads. Performance metrics include the coefficient of determination ( $R^2$ ), as well as the SDs of the residual error and watershed-level random effect distributions

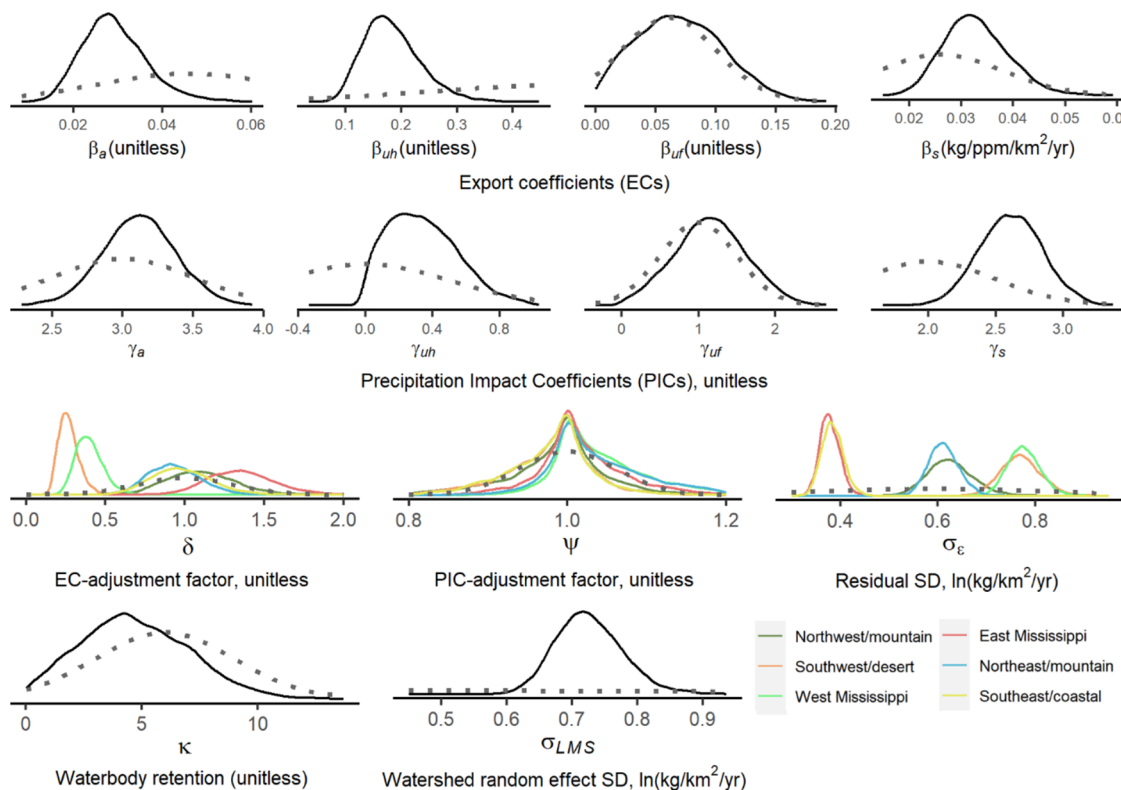


**Figure 2.** Posterior distributions for selected model parameters, along with prior distributions (dotted lines). For regional adjustment factors ( $\delta$  and  $\psi$ ) and residual SD, hyper-distributions are provided instead of priors. Note that priors and posteriors are tabulated for all parameters (including hyper-parameters) in S2.

( $\sigma_e$  and  $\sigma_{LMS}$ ). For  $R^2$ , predicted exports were calculated using the mean posterior parameter estimates, with and without the watershed-level random effect.

**2.6. Model Application to CONUS.** After calibration, we applied the model to predict TP export from 2002–2012 at the HUC8 watershed scale across CONUS. We also estimated the contribution from each P source and the fraction of anthropogenic inputs lost to watershed export. For comparison purposes, we present these findings under 10th-percentile, mean, and 90th-percentile precipitation, as determined from HUC8 precipitation data (1970–2018) and assuming anthropogenic inputs for 2012. Since <1% of precipitation values in the calibration data set are larger than 2000 mm, we capped HUC8 precipitation at this value to avoid extrapolation (see Section 3.5 for discussion).

### 3. RESULTS AND DISCUSSION

Through Bayesian inference, the model provides probabilistic estimates of various parameters that control P export (Figure 2 and Table S2–2). Based largely on these posterior parameter estimates, Sections 3.1–3.3 discuss how P export varies across space and time. Section 3.4 examines model fit, Section 3.5 presents model predictions for the entire CONUS, and Section 3.6 discusses the implications of this study.

**3.1. TP Export under Mean Precipitation.** The ECs for the anthropogenic sources (agriculture, urban fertilizer, and human waste inputs) represent the fraction of annual P inputs exported to rivers under mean precipitation conditions (Figure 2). Only about 3% of agricultural P inputs are expected to be exported to waterways, and this estimate has relatively low uncertainty, with a coefficient of variation (CV) of 0.25. In contrast, about 7% (CV = 0.50) of urban fertilizer inputs are

exported, exceeding the agricultural EC with an 87% probability (as determined by the frequency of exceedance among posterior samples). Moreover, about 18% (CV = 0.27) of human waste inputs are exported to rivers, exceeding the urban fertilizer loss rate with 97% probability. Finally, the background soil EC indicates that 0.033 kg/km<sup>2</sup>/yr of P export occurs per ppm of geogenic soil P. For the average soil P concentration of 668 ppm (across CONUS), it results in 22 kg/km<sup>2</sup>/yr of P export.

Of the anthropogenic inputs considered, agriculture has the lowest EC, likely due to crop removal. For CONUS, about 60% of the agricultural P inputs are removed with harvested crops (and in some areas, P harvest exceeds P input),<sup>26</sup> substantially reducing the P available for hydrologic export. Urban fertilizer export is about twice as high as agricultural export, consistent with the fact that urban vegetation is not systematically harvested. The relatively high EC from human waste indicates that a substantial fraction of TP from food-related and other household waste (e.g., detergents) is discharged into rivers. Note that the human waste input estimates used in this study did not include industrial P effluent,<sup>26</sup> which while expected to be small, may also influence the estimated EC. Still, the human waste EC (0.18) is generally consistent with available information on wastewater treatment. We expect around 70–95% P removal in septic systems depending on soil conditions.<sup>40</sup> Wastewater treatment plant (WWTP) removal rates vary considerably, but only a minority of WWTPs achieve effluent P of <1 mg/L.<sup>41</sup> It is also possible that a significant portion of P from human waste is exported due to leaking sewage infrastructure.<sup>42</sup>

The posterior estimate for the background soil EC was slightly larger than the prior expectation (Figure 2). In regional

SPARROW models that accounted for soil P, this variable was found to be an important source, accounting for more than 30% of P delivered to receiving waterbodies.<sup>43–45</sup> However, background soil material was not considered in many other SPARROW applications and studies that relate P inputs to P export.<sup>8,9</sup> While background soil P can be considered a natural source, its export is likely intensified through human activities that increase soil erosion rates.<sup>46</sup> Plowing, unsustainable agricultural practices (e.g., intensive tilling, overgrazing), and deforestation are the leading causes of human-induced soil erosion.<sup>47</sup> Thus, estimates of background P export could potentially be refined by considering interactions between anthropogenic activities and natural factors (e.g., soil type, slope) influencing soil erosion.

The marginal posterior distributions are generally tighter than the prior distributions, indicating that the model formulation and data effectively reduce process rate uncertainties. For ECs and PICs, SDs are reduced by 50 and 53% on average, respectively. Also, EC means shift by  $\pm 40\%$  (on average) relative to the priors. The urban fertilizer parameters are least changed from the priors, probably because urban fertilizer is a relatively small source that has limited influence on overall watershed export.

Retention in waterbodies was parametrized using a first-order exponential decay rate, and results indicate that for each 1% increase in waterbody coverage, retention increases by about 5%. Thus, for the mean water cover of 1.8% across CONUS, there is 8.2% P retention. Our retention parameter ( $\kappa$ ) is not directly comparable to SPARROW coefficients due to differences in formulation, but overall retention is compared below (Section 3.5).

**3.2. Precipitation Impacts.** PICs determine how TP export varies across the precipitation gradient. We find that agricultural inputs have the largest PIC, with relatively low uncertainty ( $CV = 0.08$ ), indicating that a 10% increase in annual precipitation (relative to the mean) will increase TP export by about 35%. Human waste inputs have the lowest PIC, resulting in only a 3% increase in TP export for a 10% increase in annual rainfall. This is consistent with human waste being collected by wastewater infrastructure, where it is less subject to hydrologic mobilization. PICs for urban fertilizer and background soils are intermediate in magnitude. There is little overlap in the posterior distributions of the four PICs, indicating that the model and data were sufficient to discriminate among these sources.

The variation in PIC estimates across different sources is generally consistent with our prior expectation. The TP watershed model calibrated by Karimi et al.<sup>13</sup> also showed a higher PIC for agriculture and a lower PIC for urban areas. This implies that in urban areas, a smaller amount of rainfall is needed to mobilize P compared to agricultural lands, where the majority of P export may occur during high precipitation conditions.<sup>48,49</sup> While we allowed export rates to vary interannually, we did not consider interannual variability in retention. A representation of how retention changes over time due to precipitation could refine our model estimates, but we do not expect retention to have as much interannual variability as nutrient export.<sup>13</sup>

Note that the ECs in this study represent export under mean precipitation conditions and not necessarily long-term mean export. Consistent with the power function used to model precipitation effects (eq 3), overall export can be heavily influenced by years of extreme precipitation. This is especially

true for agriculture, which has the largest PIC. We find a mean agricultural export fraction of 0.037 (28% higher than the agricultural EC), determined by averaging annual exports across the study period. The mean export rates for urban fertilizer, human waste, and background soil are 0.065 (fraction), 0.15 (fraction), and 0.034 (kg/ppm/km<sup>2</sup>/yr), respectively, which are closer to their corresponding EC values.

**3.3. Regional Variability.** Regional variations in export under mean precipitation are facilitated through the hierarchically modeled adjustment factors,  $\delta$ . We find the lowest  $\delta$ s for the southwest/desert and the west Mississippi regions, indicating that these regions export 73 and 60% less TP than average, respectively. In fact,  $\delta$  in the southwest/desert is smaller than the other regions (except the west Mississippi region) with >99% probability. The east Mississippi and northwest/mountain regions have the highest  $\delta$ s, indicating that these regions export 35 and 10% more than average, respectively.

The lowest values of  $\delta$  correspond to regions of low precipitation, likely due to reduced mobilization, wash-off, and instream transport of nutrients.<sup>50</sup> At the same time, these low-precipitation regions had relatively high residual error rates ( $\sigma_e$  in Table S2–2), indicating they are also less predictable. We only found one other study that systematically incorporated regional variation in model parameters.<sup>10</sup> This study used a relatively coarse partitioning into three regions and found few instances of substantial regional variability for TP parameters. On the other hand, the six regional SPARROW models<sup>9</sup> are not directly comparable due to differences in parameterization. In contrast, our consistent model formulation coupled with regional adjustment factors helps facilitate regional comparisons.

Regional variation is also accommodated using PIC adjustments,  $\psi$ . In contrast to the  $\delta$ s, these adjustments are found to be relatively small, with largely overlapping posterior distributions (Figure 2). The highest  $\psi$  (indicating a + 4% adjustment in PIC) is for the west Mississippi region, while the lowest (−2%) is for the southwest/desert and southeast/coastal regions. Considering parameter uncertainty, the probability that the west Mississippi value exceeds the southwest/desert value is just 80%. These results suggest that  $\psi$ s could potentially be omitted from the model without a substantial reduction in model performance. This might facilitate adding more influential sources of variability to the model. For example, future model iterations could consider regional adjustments for particular source types.

**3.4. Model Fit.** Model predictions can be compared to the WRTDS estimates (referred to here as “observations”) to evaluate the ability of the model to explain spatial and temporal variability in TP export. The full model, including the watershed-level random effects, explains 85% of the variability in observed TP export on the log-transformed (model) space, and 84% on the original space (Figure S3–1, top row). Discounting the watershed-level random effects, the model still explains 62 and 53% of TP export variability on the log-transformed and original scales, respectively (Figure S3–1, bottom row). These lower  $R^2$  values indicate how the model would perform if applied to a new location with no observational data. Model fit is fairly consistent across the various regions, with  $R^2$  values ranging from 0.43 to 0.57 (Figure S3–2). However, across individual LMS watersheds, model fit is more variable (Figures S3–3 and S3–4).

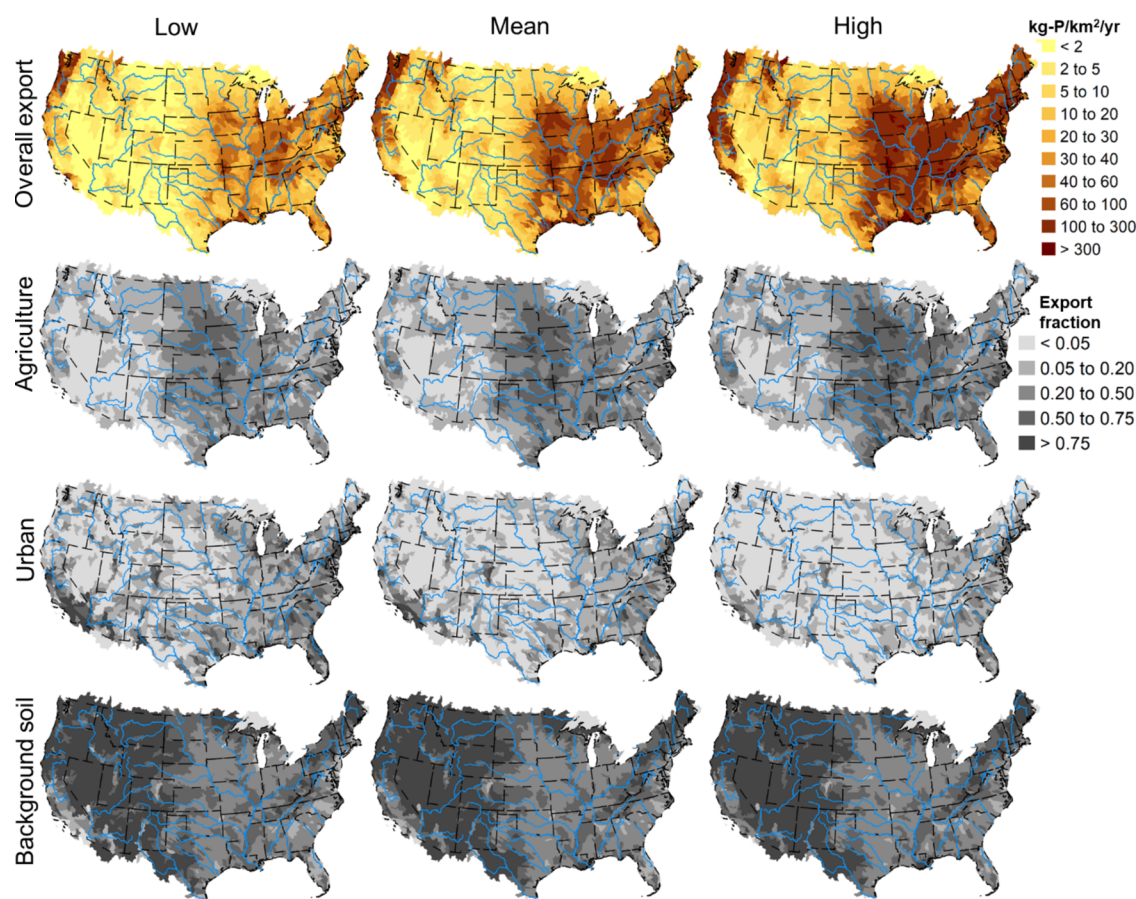


**Figure 3.** Total P export from all sources prior to waterbody retention (top) and contribution fraction from agriculture (second row), urban (third row), and background soil (bottom) under 10th-percentile (left), mean (middle) and 90th-percentile (right) precipitation conditions.

We examined model residuals and random effects for signs of temporal and spatial correlation. The average lag-1 autocorrelation coefficient across the LMS watersheds was  $-0.05$ , indicating minimal dependence between observations in consecutive years. The watershed-level random effects, which characterize spatial deviations from deterministic model predictions, do not exhibit substantial spatial correlation across CONUS (Figure S3–5). However, we found mostly positive random effects in the central MRB, particularly in agricultural regions of Missouri, Iowa, and Illinois. This indicates that more P (than expected) is lost to rivers in these LMS watersheds. Determining the reasons for this deviation is beyond the scope of this study, but it could potentially be related to differences in farming practices or geological conditions. To the extent that spatial correlation exists, it can also potentially be addressed through more complex error formulations within the hybrid watershed model.<sup>51,52</sup>

For comparison, the model can also be formulated without accounting for regional variability (without  $\psi$  and  $\delta$ ). In this case,  $R^2$  (without random effects) decreases from 62 to 48% on the log-transformed scale and from 53 to 45% on the original scale. Thus, regional adjustments contribute substantially to overall model performance.

**3.5. Application to CONUS.** TP export varies substantially across the United States and under different precipitation conditions (Figure 3, top row). As expected, we find higher TP export in more densely developed regions, including the Pacific coast and most of the eastern CONUS. The top 10% of HUC8 watersheds in terms of TP export are mostly in the central-to-

eastern MRB and along the Pacific Northwest Coast. These watersheds, which account for only 8% of the CONUS land area, account for a disproportionate 35% of CONUS TP export and also have some of the greatest year-to-year variability in TP export (Figure S3–6). TP export can also be aggregated across the entire United States. Under 10th-percentile (low), mean, and 90th-percentile (high) precipitation, the total estimated TP load is 157, 287, and 501 Gg/year, respectively, further highlighting the importance of precipitation in controlling nutrient losses. If precipitation values were not truncated at 2000 mm to avoid extrapolation of PIC relationships (Section 2.6), there would be a 1, 4, and 8% increase in total TP load for low, mean, and high precipitation, respectively, largely due to increased export along the northwest Pacific coast.

Spatial variation in TP export (Figure 3) is largely explained by anthropogenic inputs and background P sources. We find high TP export throughout a large portion of the central and eastern MRB, where agriculture is a dominant source of P (Figure S1–2). High TP export in the Pacific Northwest is explained, in part, by high background soil P (Figure S1–3). Other coastal regions have high TP export largely due to urban or a combination of agricultural and urban inputs. Areas of high export are reasonably consistent with the regional SPARROW models,<sup>9</sup> where the highest TP export was found in the lower Missouri and Mississippi River basins.

We find considerable variability in waterbody TP retention across CONUS (Figure S3–7). On average, 8% of TP is retained within waterbodies. Higher retention rates (>85%) are



**Figure 4.** Percent of anthropogenic (agricultural and urban) P inputs that are exported to waterways (prior to waterbody retention) under low (left), mean (middle), and high (right) precipitation condition.

estimated for watersheds with large lakes, such as the Great Salt Lake and Lake Tahoe. Low waterbody retention (<1%) generally occurs in arid western regions of CONUS. We note that some SPARROW models suggest higher retention, such as >30% retention in streams and waterbodies in the upper MRB,<sup>12</sup> whereas we find an average of 13% retention in waterbodies for this region. While all such estimates are subject to uncertainty, our retention formulation could potentially be refined to consider stream losses and additional waterbody attributes, such as reservoir hydraulic loading rates.<sup>11</sup>

Spatial patterns in TP source apportionment vary across different watersheds and precipitation conditions (rows 2–4 of Figure 3). Agricultural inputs account for >50% of TP export in 16% of U.S. lands, mainly in the MRB and southeast states, where agricultural inputs are high. This area drops to 9% under low precipitation conditions and increases to 24% under high precipitation conditions. On the other hand, urban (urban fertilizer plus human waste) inputs account for >50% of TP export in only about 6% of the CONUS, located mainly in populated coastal areas. Under high and low precipitation conditions, this area changes to 3 and 12%, respectively. Comparing the two urban sources reveals that human waste greatly exceeds urban fertilizer export (Figure S3–8).

Finally, background soil P accounts for >50% of TP export in about 60% of the CONUS under all precipitation conditions. On average, background soil P makes up 49% of the CONUS-wide TP export. It is particularly important in areas with low anthropogenic inputs and high soil P concentrations, which is generally consistent with previous modeling studies that account for this source type.<sup>43,44</sup> For example, geologic material was found to be the source of more than 90% of the TP load in the Pacific Northwest.<sup>45</sup>

A benefit of formulating our model in terms of net TP inputs is that it allows a direct determination of the fraction of these inputs lost to hydrologic export. Under mean precipitation, 4.2% (CV = 0.24) of all anthropogenic inputs are being exported to waterways, which decreases to 2.7% and increases to 7.0% during low and high precipitation, respectively. There is also substantial spatial variability in the fraction of anthropogenic P inputs lost to watershed export (Figure 4), varying from 0.02–31% under mean precipitation. Higher export fractions are generally associated with regions of higher precipitation, such as the Pacific Northwest coast and southern MRB. As precipitation increases to the 90th-percentile, more watersheds in these areas export >10% of anthropogenic inputs, while most of the watersheds in the arid west still export less <2% of inputs.

Agriculture shows the greatest variability in export fraction due to precipitation, consistent with its high PIC. Under mean precipitation, 3.0% of agricultural inputs are exported,

increasing to 6.0% under high precipitation, and dropping to 1.4% under low precipitation. The export fraction varies less for urban inputs. Under low, mean, and high precipitation, urban inputs are exported at rates of 11.2, 12.2, and 13.2%, respectively. Other studies have also found that the export of nutrient inputs is largely explained by variations in climate.<sup>53,54</sup> These studies found a positive linear or exponential relationship between precipitation and the fraction of anthropogenic input exported. Higher precipitation enhances leakage from sewers, septic systems, and fertilizer runoff that exacerbate the export of P inputs.<sup>55</sup> Also, P accumulated over long periods (i.e., legacy P) can potentially be remobilized and transported to rivers, particularly during wet years.<sup>56,57</sup> Thus, estimates of legacy P could be considered in future model refinements.

In some studies, export fractions are determined relative to the net anthropogenic phosphorus input (NAPI), which sums up the inputs from agricultural and human sources and subtracts crop removal. Combining our inputs and accounting for crop removal<sup>26</sup> shows that about 7.7% of the NAPI (CV = 0.12) is exported across CONUS under mean precipitation, which reduces to 6.9% after accounting for waterbody retention. We note the percent NAPI lost to rivers varies widely across studies, with estimates ranging from 2–15% across major watersheds in North America<sup>58–60</sup> and Europe.<sup>54</sup>

**3.6. Implications.** The model developed here characterizes P export as a function of both anthropogenic inputs and background soil P. This is especially important in large-scale nutrient budgets since estimates of the fraction of anthropogenic inputs lost to riverine export are usually unavailable and assumed low.<sup>26</sup> Here, we find that over 5% of anthropogenic inputs are likely to be exported to waterways throughout much of the United States, and this export increases substantially under high precipitation conditions (Figure 4). We also determine the fraction of P lost for individual inputs (i.e., agriculture, urban fertilizer, and human waste) rather than as a composite (e.g., NAPI). This can help policymakers prioritize management of different P sources and improve P use efficiency across different sectors. In addition, identifying hotspots of P export spatially and under different precipitation conditions can help managers target limited resources toward particular watersheds.<sup>7</sup> The approach can also be transferred to other areas (i.e., other nations or continents), and the Bayesian hierarchical formulation may be particularly beneficial for accommodating regions with sparse data, as the model incorporates prior knowledge from previous research and partially pools available data across regions.<sup>10,15,16</sup>

We find that precipitation greatly impacts the fraction of anthropogenic inputs lost to waterways. Previous studies have also shown the effects of precipitation on the fraction of NAPI exported. However, these studies were developed for smaller

areas, and the export fraction was typically compared to climatological variables through post hoc analyses.<sup>53,54,61</sup> Here, for the first time, we directly integrated precipitation into a large-scale model that characterizes P losses from different sources. We show that agriculture is particularly sensitive to precipitation conditions, with 6% of annual agricultural inputs lost to riverine export under 90th-percentile precipitation.

Results also emphasize the importance of background (geogenic) soil P, as it is found to be the dominant source of exported P throughout a majority of the CONUS land area, and it typically accounts for >20% of exported P even in watersheds with intensive agriculture. Thus, P from natural sources needs to be considered when developing comprehensive nutrient budgets. Furthermore, water quality management strategies should consider controls on background P export, which is likely exacerbated by erosion from anthropogenic activities. Related to this, future research could explore how loading rates for different forms of P (e.g., particulate versus dissolved) vary across different regions and hydrologic conditions.<sup>62,63</sup>

Finally, this study demonstrates the effectiveness of the hybrid Bayesian approach in explaining nutrient fluxes across large spatial and temporal scales. This was facilitated, in part, through the regionalization of key rates within a hierarchical framework. The model demonstrates a proof of concept for capturing broad-scale patterns in nutrient export and the fraction of anthropogenic inputs exported. It can potentially be expanded in the future to consider more complex loading and retention formulations, as discussed previously (Sections 3.1, 3.2, and 3.5), and the regionalization of additional parameters used in these formulations. In addition, incorporating factors such as extreme precipitation and temperature, which might also affect interannual variability in P export,<sup>6,8</sup> could be considered within the context of the hybrid model. To prevent overparameterization, such model enhancements could potentially be facilitated through an expanded calibration data set or more precise prior knowledge of relevant loading and retention rates.

## ASSOCIATED CONTENT

### Data Availability Statement

Model inputs can be obtained from the public sources described in the methods. The processed data sets and codes (sufficient to run the model) are available at [10.5281/zenodo.10622215](https://doi.org/10.5281/zenodo.10622215).

### Supporting Information

The Supporting Information is available free of charge at <https://pubs.acs.org/doi/10.1021/acs.est.3c07479>.

Model inputs; parameter estimates; model performance; and the spatiotemporal variability in TP export ([PDF](#))

## AUTHOR INFORMATION

### Corresponding Author

**Kimia Karimi** – *Center for Geospatial Analytics, North Carolina State University, Raleigh, North Carolina 27695, United States*; [orcid.org/0000-0003-3750-4221](https://orcid.org/0000-0003-3750-4221); Email: [kkarimi2@ncsu.edu](mailto:kkarimi2@ncsu.edu)

### Author

**Daniel R. Obenour** – *Center for Geospatial Analytics, North Carolina State University, Raleigh, North Carolina 27695, United States; Department of Civil, Construction and*

*Environmental Engineering, North Carolina State University, Raleigh, North Carolina 27606, United States*; [orcid.org/0000-0002-7459-218X](https://orcid.org/0000-0002-7459-218X)

Complete contact information is available at: <https://pubs.acs.org/10.1021/acs.est.3c07479>

### Notes

The authors declare no competing financial interest.

## ACKNOWLEDGMENTS

This research was funded by the Science and Technologies for Phosphorus Sustainability (STEPS) Center, a National Science Foundation Science and Technology Center (CBET-2019435). The authors thank Sankar Arumugam, Smitom Borah, Owen Duckworth, Rebecca Muenich, Natalie Nelson, Paul Westerhoff, and three anonymous reviewers for providing valuable project and manuscript feedback.

## REFERENCES

- (1) Brooks, B. W.; Lazorchak, J. M.; Howard, M. D. A.; Johnson, M. V. V.; Morton, S. L.; Perkins, D. A. K.; Reavie, E. D.; Scott, G. I.; Smith, S. A.; Steevens, J. A. Are harmful algal blooms becoming the greatest inland water quality threat to public health and aquatic ecosystems? *Environ. Toxicol. Chem.* **2016**, *35* (1), 6–13.
- (2) Howarth, R. W.; Anderson, D. B.; Cloern, J. E.; Elfring, C.; Hopkinson, C. S.; Lapointe, B.; Malone, T.; Marcus, N.; McGlathery, K.; Sharpley, A. N.; Walker, D. Nutrient pollution of coastal rivers, bays, and seas. *Issues Ecol.* **2000**, *7*, 1–16.
- (3) Carpenter, S. R. Phosphorus control is critical to mitigating eutrophication. *Proc. Natl. Acad. Sci. U.S.A.* **2008**, *105* (32), 11039–11040.
- (4) Schindler, D. W.; Carpenter, S. R.; Chapra, S. C.; Hecky, R. E.; Orihel, D. M. Reducing phosphorus to curb lake eutrophication is a success. *Environ. Sci. Technol.* **2016**, *50* (17), 8923–8929.
- (5) Del Giudice, D.; Fang, S.; Scavia, D.; Davis, T. W.; Evans, M. A.; Obenour, D. R. Elucidating controls on cyanobacteria bloom timing and intensity via Bayesian mechanistic modeling. *Sci. Total Environ.* **2021**, *755*, No. 142487.
- (6) Sinha, E.; Michalak, A. M. Precipitation dominates interannual variability of riverine nitrogen loading across the continental United States. *Environ. Sci. Technol.* **2016**, *50* (23), 12874–12884.
- (7) Sabo, R. D.; Clark, C. M.; Compton, J. E. Considerations when using nutrient inventories to prioritize water quality improvement efforts across the U.S. *Environ. Res. Commun.* **2021**, *3* (4), No. 045005, DOI: [10.1088/2515-7620/abf296](https://doi.org/10.1088/2515-7620/abf296).
- (8) Huo, S.; Ma, C.; Li, W.; He, Z.; Zhang, H.; Yu, L.; Liu, Y.; Cao, X.; Wu, F. Spatiotemporal differences in riverine nitrogen and phosphorus fluxes and associated drivers across China from 1980 to 2018. *Chemosphere* **2023**, *310*, No. 136827, DOI: [10.1016/j.chemosphere.2022.136827](https://doi.org/10.1016/j.chemosphere.2022.136827).
- (9) Preston, S. D.; Alexander, R. B.; Schwarz, G. E.; Crawford, C. G. Factors affecting stream nutrient loads: a synthesis of regional SPARROW model results for the continental United States. *J. Am. Water Resour. Assoc.* **2011**, *47* (5), 891–915.
- (10) Schwarz, G. E.; Alexander, R. B.; Smith, R. A.; Preston, S. D. The regionalization of national-scale SPARROW models for stream nutrients. *J. Am. Water Resour. Assoc.* **2011**, *47* (5), 1151–1172.
- (11) Smith, R. A.; Schwarz, G. E.; Alexander, R. B. Regional interpretation of water-quality monitoring data. *Water Resour. Res.* **1997**, *33* (12), 2781–2798.
- (12) Alexander, R. B.; Smith, R. A.; Schwarz, G. E. Estimates of diffuse phosphorus sources in surface waters of the United States using a spatially referenced watershed model. *Water Sci. Technol.* **2004**, *49* (3), 1–10.
- (13) Karimi, K.; Miller, J. W.; Sankarasubramanian, A.; Obenour, D. R. Contrasting annual and summer phosphorus export using a hybrid

- Bayesian watershed model. *Water Resour. Res.* **2023**, *59* (1), No. e2022WR033088.
- (14) Wellen, C.; Arhonditsis, G. B.; Labencki, T.; Boyd, D. A Bayesian methodological framework for accommodating interannual variability of nutrient loading with the SPARROW model. *Water Resour. Res.* **2012**, *48* (10), DOI: 10.1029/2012WR011821.
- (15) Gelman, A.; Hill, J. *Data Analysis Using Regression and Multilevel/Hierarchical Models*; Cambridge University Press, 2006.
- (16) Alexander, R. B.; Schwarz, G. E.; Boyer, E. W. Advances in quantifying streamflow variability across continental scales: 2. improved model regionalization and prediction uncertainties using hierarchical Bayesian methods. *Water Resour. Res.* **2019**, *55* (12), 11061–11087.
- (17) Gelman, A.; Carlin, J. B.; Stern, H. S.; Rubin, D. B. *Bayesian Data Analysis*; CRC, 2014.
- (18) Strickling, H. L.; Obenour, D. R. Leveraging spatial and temporal variability to probabilistically characterize nutrient sources and export rates in a developing watershed. *Water Resour. Res.* **2018**, *54* (7), 5143–5162.
- (19) USGS. USGS water data for the Nation: US Geological Survey National Water Information System database; U.S. Geological Survey, 2022. <http://dx.doi.org/10.5066/F7P5SKJN>.
- (20) IBWC.Rio Grande Historical Mean Daily Discharge Data; International Boundary & Water Commission: United States and Mexico, 2022. [https://www.ibwc.gov/Water\\_Data/rio\\_grande\\_WF.html#Stream](https://www.ibwc.gov/Water_Data/rio_grande_WF.html#Stream).
- (21) NWQMC.Water Quality Portal; National Water Quality Monitoring Council, 2022. <https://www.waterqualitydata.us>
- (22) NCWQR. Heidelberg Tributary Loading Program (HTLP) Dataset; National Center for Water Quality Research, 2022. <https://doi.org/10.5281/zenodo.6606949>.
- (23) Hirsch, R. M.; Moyer, D. L.; Archfield, S. A. Weighted regressions on time, discharge, and season (WRTDS), with an application to chesapeake bay river inputs. *J. Am. Water Resour. Assoc.* **2010**, *46* (5), 857–880.
- (24) Falcone, J. A.; Carlisle, D. M.; Wolock, D. M.; Meador, M. R. GAGES: A stream gage database for evaluating natural and altered flow conditions in the conterminous United States. *Ecology* **2010**, *91* (2), No. 621, DOI: 10.1890/09-0889.1.
- (25) USGS. The StreamStats program; U.S. Geological Survey (USGS), 2019.
- (26) Sabo, R. D.; Clark, C. M.; Gibbs, D. A.; Metson, G. S.; Todd, M. J.; LeDuc, S. D.; Greiner, D.; Fry, M. M.; Polinsky, R.; Yang, Q.; Tian, H.; Compton, J. Phosphorus inventory for the conterminous United States (2002–2012). *J. Geophys. Res.: Biogeosci.* **2021**, *126* (4), No. e2020JG005684.
- (27) Tipping, E.; Benham, S.; Boyle, J. F.; Crow, P.; Davies, J.; Fischer, U.; Guyatt, H.; Helliwell, R.; Jackson-Blake, L.; Lawlor, A. J.; Montheith, D. T.; Rowe, E. C.; Toberman, H. Atmospheric deposition of phosphorus to land and freshwater. *Environ. Sci.: Process Impacts* **2014**, *16* (7), 1608–1617.
- (28) Falcone, J. A. *US Block-Level Population Density Rasters for 1990, 2000, and 2010*; U.S. Geological Survey, 2016.
- (29) Falcone, J. A. *U.S. conterminous wall-to-wall anthropogenic land use trends (NWALT)*, 1974–2012.; U.S. Geological Survey, 2015. <http://pubs.er.usgs.gov/publication/ds948>.
- (30) CEC. *North American Environmental Atlas*; Commission for Environmental Cooperation, 2022. [http://www.cec.org/north-american-environmental-atlas/?\\_atlas\\_search=LANDCOVER](http://www.cec.org/north-american-environmental-atlas/?_atlas_search=LANDCOVER).
- (31) Smith, D. B.; Cannon, W. F.; Woodruff, L. G.; Solano, F.; Kilburn, J. E.; Fey, D. L. *Geochemical and Mineralogical Data for Soils of the Conterminous United States*; U.S. Geological Survey, 2013. <https://pubs.usgs.gov/ds/801/>.
- (32) Woodruff, L.; Cannon, W. F.; Smith, D. B.; Solano, F. The distribution of selected elements and minerals in soil of the conterminous United States. *J. Geochem. Explor.* **2015**, *154*, 49–60.
- (33) PRISM Climate Group, Oregon State University, 2022. <http://prism.oregonstate.edu>.
- (34) Smith, N. J.; Webster, K. E.; Rodriguez, L. K.; Cheruvelil, K. S.; Soranno, P. A. LAGOS-US GEO v1. 0: Data module of lake geospatial ecological context at multiple spatial and temporal scales in the conterminous US. <https://doi.org/10.6073/pasta/0e443bd43d7e24c2b6abc7af54ca424a>.
- (35) Brett, M. T.; Benjamin, M. M. A review and reassessment of lake phosphorus retention and the nutrient loading concept. *Freshwater Biol.* **2008**, *53* (1), 194–211.
- (36) Bernhardt, E. S. Cleaner lakes are dirtier lakes. *Science* **2013**, *342* (6155), 205–206.
- (37) Neal, R. M. MCMC using Hamiltonian dynamics. In *Handbook of Markov Chain Monte Carlo*; CRC, 2011.
- (38) Stan Development Team. R Stan: the R interface to Stan. 2020. <http://mc-stan.org/>.
- (39) R Core Team. R: *A Language and Environment for Statistical Computing*; R Foundation for Statistical Computing, 2022. <https://www.r-project.org/>.
- (40) Robertson, W. D.; Van Stempvoort, D. R.; Schiff, S. L. Review of phosphorus attenuation in groundwater plumes from 24 septic systems. *Sci. Total Environ.* **2019**, *692*, 640–652.
- (41) EPA. National Study of Nutrient Removal and Secondary Technologies; U.S. Environmental Protection Agency, 2023. <https://www.epa.gov/eg/national-study-nutrient-removal-and-secondary-technologies#fact-sheets>.
- (42) Pennino, M. J.; Kaushal, S. S.; Mayer, P. M.; Utz, R. M.; Cooper, C. A. Stream restoration and sewers impact sources and fluxes of water, carbon, and nutrients in urban watersheds. *Hydro. Earth Syst. Sci.* **2016**, *20* (8), 3419–3439.
- (43) Domagalski, J.; Saleh, D. Sources and transport of phosphorus to rivers in California and adjacent states, U.S., as determined by SPARROW modeling. *J. Am. Water Resour. Assoc.* **2015**, *51* (6), 1463–1486.
- (44) García, A. M.; Hoos, A. B.; Terziotti, S. A regional modeling framework of phosphorus sources and transport in streams of the southeastern United States. *J. Am. Water Resour. Assoc.* **2011**, *47* (5), 991–1010.
- (45) Wise, D. R.; Johnson, H. M. Surface-water nutrient conditions and sources in the United States Pacific Northwest. *J. Am. Water Resour. Assoc.* **2011**, *47* (5), 1110–1135.
- (46) Nearing, M. A.; Xie, Y.; Liu, B.; Ye, Y. Natural and anthropogenic rates of soil erosion. *Int. Soil Water Conserv. Res.* **2017**, *5* (2), 77–84.
- (47) Borrelli, P.; Robinson, D. A.; Panagos, P.; Lugato, E.; Yang, J. E.; Alewell, C.; Wuepper, D.; Montanarella, L.; Ballabio, C. Land use and climate change impacts on global soil erosion by water (2015–2070). *Proc. Natl. Acad. Sci. U.S.A.* **2020**, *117* (36), 21994–22001.
- (48) Banner, E. B. K.; Stahl, A. J.; Dodds, W. K. Stream discharge and riparian land use influence In-stream concentrations and loads of phosphorus from central plains watersheds. *Environ. Manage.* **2009**, *44* (3), 552–565.
- (49) Shields, C. A.; Band, L. E.; Law, N.; Groffman, P. M.; Kaushal, S. S.; Savvas, K.; Fisher, G. T.; Belt, K. T. Streamflow distribution of non-point source nitrogen export from urban-rural catchments in the Chesapeake Bay watershed. *Water Resour. Res.* **2008**; Vol. 44 9 DOI: 10.1029/2007WR006360.
- (50) Haith, D. A.; Shoemaker, L. L. Generalized watershed loading functions for stream flow nutrients. *J. Am. Water Resour. Assoc.* **1987**, *23* (3), 471–478.
- (51) Qian, S. S.; Reckhow, K. H.; Zhai, J.; McMahon, G. Nonlinear regression modeling of nutrient loads in streams: A Bayesian approach. *Water Resour. Res.* **2005**, *41* 7, DOI: 10.1029/2005WR003986.
- (52) Peterson, E. E.; Merton, A. A.; Theobald, D. M.; Urquhart, N. S. Patterns of spatial autocorrelation in stream water chemistry. *Environ. Monit. Assess.* **2006**, *121* (1–3), 571–596.
- (53) Chen, D.; Hu, M.; Guo, Y.; Dahlgren, R. A. Influence of legacy phosphorus, land use, and climate change on anthropogenic phosphorus inputs and riverine export dynamics. *Biogeochemistry* **2015**, *123* (1–2), 99–116.

- (54) Hong, B.; Swaney, D. P.; Mört, C. M.; Smedberg, E.; Hägg, H. E.; Humborg, C.; Howarth, R. W.; Bouraoui, F. Evaluating regional variation of net anthropogenic nitrogen and phosphorus inputs (NANI/NAPI), major drivers, nutrient retention pattern and management implications in the multinational areas of Baltic Sea basin. *Ecol. Modell.* **2012**, *227*, 117–135.
- (55) Morse, N. B.; Wollheim, W. M. Climate variability masks the impacts of land use change on nutrient export in a suburbanizing watershed. *Biogeochemistry* **2014**, *121* (1), 45–59.
- (56) Han, H.; Allan, J. D.; Scavia, D. Influence of climate and human activities on the relationship between watershed nitrogen input and river export. *Environ. Sci. Technol.* **2009**, *43* (6), 1916–1922.
- (57) Van Meter, K. J.; McLeod, M. M.; Liu, J.; Tenkouano, G. T.; Hall, R. I.; Van Cappellen, P.; Basu, N. B. Beyond the mass balance: watershed phosphorus legacies and the evolution of the current water quality policy challenge. *Water Resour. Res.* **2021**, *57* (10), No. e2020WR029316.
- (58) Stackpole, S.; Sabo, R.; Falcone, J.; Sprague, L. Long-term Mississippi River trends expose shifts in the river load response to watershed nutrient balances between 1975 and 2017. *Water Resour. Res.* **2021**, *57* (11), No. e2021WR030318.
- (59) Goyette, J. O.; Bennett, E. M.; Howarth, R. W.; Maranger, R. Changes in anthropogenic nitrogen and phosphorus inputs to the St. Lawrence sub-basin over 110 years and impacts on riverine export. *Global Biogeochem. Cycles* **2016**, *30* (7), 1000–1014.
- (60) Russell, M. J.; Weller, D. E.; Jordan, T. E.; Sigwart, K. J.; Sullivan, K. J. Net anthropogenic phosphorus inputs: Spatial and temporal variability in the Chesapeake Bay region. *Biogeochemistry* **2008**, *88* (3), 285–304.
- (61) Chen, D.; Hu, M.; Wang, J.; Guo, Y.; Dahlgren, R. A. Factors controlling phosphorus export from agricultural/forest and residential systems to rivers in eastern China, 1980–2011. *J. Hydrol.* **2016**, *533*, 53–61.
- (62) Uusitalo, R.; Turtola, E.; Puustinen, M.; Paasonen-Kivekäs, M.; Usi-Kämpä, J. Contribution of particulate phosphorus to runoff phosphorus bioavailability. *J. Environ. Qual.* **2003**, *32* (6), 2007–2016.
- (63) Clark, G. M.; Mueller, D. K.; Mast, M. A. Nutrient concentrations and yields in undeveloped stream basins of the United States. *J. Am. Water Resour. Assoc.* **2000**, *36* (4), 849–860.